

### Conclusion

(*N*-(*p*-Toluenesulfonyl)imino)phenyliodinane appears to react with the heme iron of cytochrome P-450 to form a transient iron(V)-nitrene complex. With the substrates studied here (cyclohexane, methylcyclohexane, *p*-xylene) the nitrene complex undergoes hydrolysis to the corresponding iron(V)-oxo complex before transfer of the nitrene to a C-H bond of the substrate can occur. The iron-oxo complex is able to attack substrate, with hydroxylation being the net result. The synthetic metalloporphyrins upon which these enzymatic studies are based should be examined to determine if the nitrene hydrolysis is part of the normal chemistry of such species or if it represents a unique

catalytic property of cytochrome P-450.

**Acknowledgment.** We thank Dr. Stephen G. Sligar for initially bringing to our attention the model work on iminiodinane nitrenoid reagents. We thank Dr. John B. Schenkman for the use of the gas chromatograph-mass spectrometer in his laboratory. This work was supported by Research Grant GM28737 from the National Institutes of Health and by the University of Connecticut Research Foundation.

**Registry No.** 1, 55962-05-5; CHP, 80-15-9; PhI=O, 536-80-1; cytochrome P-450, 9035-51-2; cyclohexane, 110-82-7; methylcyclohexane, 108-87-2; *p*-xylene, 106-42-3.

## Acid-Base Catalysis of the Elimination and Isomerization Reactions of Triose Phosphates

John P. Richard

Contribution from the Institute for Cancer Research, Fox Chase Cancer Center, Philadelphia, Pennsylvania 19111. Received December 27, 1983

**Abstract:** The nonenzymatic  $\beta$ -elimination, isomerization, and racemization reactions of L-glyceraldehyde 3-phosphate (LGAP) are through a common enediolate intermediate which partitions between leaving group expulsion, C-1 protonation, and C-2 protonation, respectively. The elimination reaction mechanisms of LGAP and dihydroxyacetone phosphate (DHAP) are E1cb because enolate intermediates have been identified in very closely related systems.<sup>13,14</sup> Strong general base catalysis of elimination demonstrates that the enediolate intermediate is formed essentially irreversibly by rate-determining substrate deprotonation. The pH rate profile for the elimination reaction of LGAP is first order in hydroxide at pH >10 due to direct substrate deprotonation by hydroxide, pH independent at pH 6-10 due to intramolecular deprotonation by the C-3 phosphate dianion, and first order in hydroxide at pH <6 due to a decrease in the reactive phosphate dianion form of the substrate. The Brønsted  $\beta$  values for buffer catalysis of DHAP and LGAP elimination by 3-substituted quinuclidines are 0.48 and 0.45, respectively. The solvent deuterium isotope effect on the second-order rate constant for quinuclidinone catalysis of DHAP elimination is 1.1. At >0.2 M concentrations of 3-oxo- and 3-hydroxy-substituted quinuclidine buffers there is curvature in the buffer catalysis plots for the elimination reaction of DHAP which is attributed to a change from rate determining substrate deprotonation to partially rate determining leaving group expulsion. The isomerization and racemization reactions of LGAP were followed by coupling the formation of DHAP and DGAP to enzymatic NADH oxidation under conditions where >90% of the product is from the elimination reaction. Uncatalyzed racemization is five times slower than uncatalyzed isomerization, and buffer-catalyzed racemization is estimated to be >20 times slower than buffer-catalyzed isomerization. The observed rate constant for LGAP isomerization is second order in total buffer concentration; the basic form of the buffer acts to increase the steady-state concentration of the enediolate, and the acidic form of the buffer increases the fractional partitioning of the enediolate to DHAP. Rate constant ratios  $k_{\text{BH}}/k_e$  and  $k_{-0}/k_e$  for partitioning of the enediolate between buffer-catalyzed or uncatalyzed protonation ( $k_{\text{BH}}$  or  $k_{-0}$ ) and leaving group expulsion ( $k_e$ ) were obtained from the slopes and the intercepts respectively of linear plots of the isomerization/elimination rate constant ratio against buffer concentration. The Brønsted  $\alpha$  value for enediolate protonation at C-1 is 0.47. The  $(k_{\text{BH}}/k_e)_{\text{H}_2\text{O}}/(k_{\text{BD}}/k_e)_{\text{D}_2\text{O}}$  ratio for quinuclidinium catalysis in  $\text{H}_2\text{O}$  and  $\text{D}_2\text{O}$  is 3.2. The pH dependence plot of  $k_{\text{BH}}/k_e$  values shows pH-independent regions at pH <7 and >10, with a 100-fold greater limiting  $k_{\text{BH}}/k_e$  value at pH >10. The increased  $k_{\text{BH}}/k_e$  value at high pH is due to slower leaving group expulsion from the enediolate phosphate dianion compared to that of the enediolate phosphate monoanion. The nonenzymatic reactions of triose phosphates are compared with the enzymatic reactions catalyzed by triose phosphate isomerase and methylglyoxal synthase.

Triose phosphates undergo isomerization and elimination reactions in water,<sup>1,2</sup> and it has been proposed that these reactions are through the enediolate intermediate formed by substrate deprotonation (eq 1).<sup>3</sup> The reversible isomerization and the irreversible elimination reactions of dihydroxyacetone phosphate are catalyzed by the enzymes triose phosphate isomerase<sup>4</sup> and methylglyoxal synthase,<sup>5</sup> respectively.

In this paper we present a study of dihydroxyacetone phosphate (DHAP) and L-glyceraldehyde 3-phosphate (LGAP) isomerization and elimination in water. In contrast to past studies of this system<sup>1-3</sup> which report observed isomerization or elimination rate constants for single sets of reaction conditions, we have determined the uncatalyzed, hydroxide-catalyzed, and buffer-catalyzed components of these rate constants over a wide pH range.

This work was initiated primarily to obtain a good estimate of the rate acceleration for the triose phosphate isomerase catalyzed

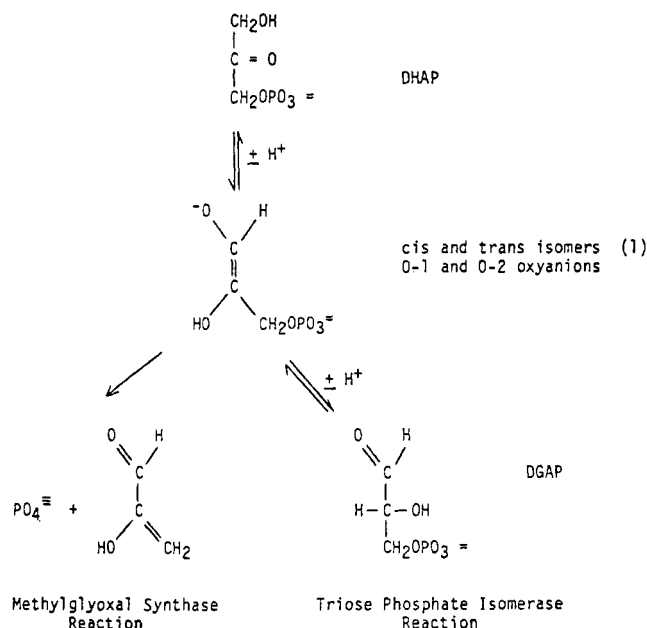
(1) Hall, A.; Knowles, J. R. *Biochemistry* **1975**, *14*, 4348.

(2) Bonsignore, A.; Leoncini, G.; Siri, A.; Ricci, D. *Ital. J. Biochem.* **1973**, *22*, 131.

(3) Iyengar, R.; Rose, I. A. *J. Am. Chem. Soc.* **1983**, *105*, 3301.

(4) Noltmann, E. A. In "The Enzymes", Boyer, P. D., Ed.; Academic Press: New York, 1972; Vol. 6, pp 271-354.

(5) (a) Hopper, D. J.; Cooper, R. A. *Biochem. J.* **1972**, *128*, 321. (b) Tsai, P. K.; Gracy, R. W. *J. Biol. Chem.* **1976**, *251*, 364. (c) Cooper, R. A. *Eur. J. Biochem.* **1974**, *44*, 81. (d) Summers, M. C.; Rose, I. A. *J. Am. Chem. Soc.* **1977**, *99*, 4475.



reaction. A rate acceleration was estimated previously on the basis of the rate constant for uncatalyzed nonenzymatic isomerization.<sup>1</sup> However, the mechanism for enzymatic isomerization involves general base-acid catalysis of carbon deprotonation-protonation by an enzyme glutamate residue,<sup>4</sup> and a more interesting estimation of the enzymatic rate acceleration would be one based on the rate constants for buffer- (general base-acid) catalyzed isomerization. We report here a comparison of rate constants for buffer- and enzyme-catalyzed triose phosphate isomerization through an enediolate intermediate.

## Materials and Methods

**Materials.** The enzymes *E. Coli* glycerokinase and yeast alcohol dehydrogenase were obtained from Sigma; rabbit muscle  $\alpha$ -glycerol-phosphate dehydrogenase (170 units/mg), rabbit muscle D-glyceraldehyde 3-phosphate dehydrogenase, and yeast 3-phosphoglycerate kinase from Boehringer; and rabbit muscle triose phosphate isomerase from Calbiochem-Behring. Enzymes obtained as  $(\text{NH}_4)_2\text{SO}_4$  precipitates were dialyzed overnight at 5 °C against 60 mM triethanolamine-HCl, pH 7.6, prior to their use.

The acetal and ketal of D,L-GAP and DHAP, respectively, were obtained from Calbiochem-Behring and were converted to the aldehyde or ketone by acid hydrolysis.<sup>6</sup> L-Glyceraldehyde and dihydroxyacetone were purchased from Aldrich and used without further purification. Substituted quinuclidines were purchased from Aldrich, converted to the hydrochloride form when necessary, and recrystallized from EtOH/H<sub>2</sub>O. Imidazole was from Sigma and was recrystallized from benzene. Triethylamine was from Aldrich, and was redistilled. Trifluoroethanol (Gold Label Grade from Aldrich), triethanolamine, and deuterium oxide were from Aldrich and were used without further purification. All inorganic compounds were reagent grade and were used without further purification, and the water was distilled and deionized. [<sup>32</sup>P]P<sub>i</sub> was from New England Nuclear.

[<sup>32</sup>P]ATP was prepared enzymatically from ADP and [<sup>32</sup>P]P<sub>i</sub> with D-Glyceraldehyde-3-phosphate dehydrogenase and 3-phosphoglycerate kinase.<sup>7</sup>

[<sup>32</sup>P]LGAP and [<sup>32</sup>P]DHAP were prepared by glycerokinase catalyzed phosphorylation of L-glyceraldehyde or dihydroxyacetone with [<sup>32</sup>P]-ATP.<sup>3</sup> The product, in 0.2 M TCA, was neutralized with KOH before being used, if the final TCA concentration was expected to be great enough to change the pH of the reaction mixture.

**Methods.** Inorganic phosphate concentrations were determined colorimetrically.<sup>8</sup> The concentrations of DGAP and DHAP were determined enzymatically by published methods,<sup>3</sup> and the total GAP concentration was determined as alkaline labile phosphate.<sup>3</sup> Unlabeled LGAP was prepared by enzymatic resolution of a mixture of D,L-GAP with D-glyceraldehyde-3-phosphate dehydrogenase. The reaction mixture was

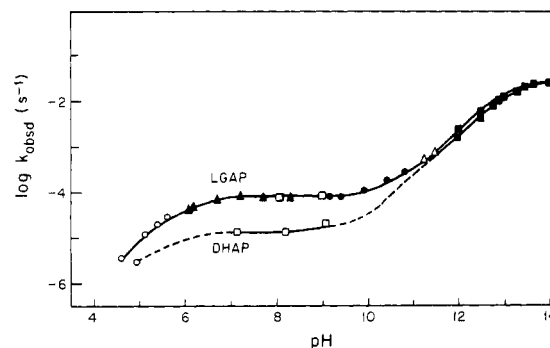


**Figure 1.** The pH rate profiles for the elimination reaction of LGAP (upper curve) and DHAP (lower curve) at 37 °C and ionic strength of 1.0 (KCl). When there is buffer catalysis the  $k_{\text{obsd}}$  values are obtained by extrapolation to zero buffer concentration. Key: ■, OH<sup>-</sup>; △, triethylamine buffer; ●, carbonate buffer; □, triethanolamine buffer; ▲, imidazole buffer; ○, acetate buffer.

prepared to a volume of 400 mL at pH 7.1 and contained: 50 mM triethanolamine hydrochloride, 0.5 mM Na<sub>2</sub>HAsO<sub>4</sub>, 1 mM ADP, 1 mM MgCl<sub>2</sub>, 18 mM acetaldehyde, 0.2 mM NAD<sup>+</sup>, 7 mM D,L-GAP, 40 mg of D-glyceraldehyde-3-phosphate dehydrogenase, 10 mg of 3-phosphoglycerate kinase, and 10 mg of alcohol dehydrogenase. The ADP and 3-phosphoglycerate kinase were added to minimize levels of contaminating phosphate. The reaction was monitored by following the change in GAP concentration. This decreased to one-half the initial value after 30–40 min, and at this time the material was applied to a 3 × 40 cm column of Dowex-1, chloride form, previously equilibrated with water. The column was washed with 1 L of water and 0.5 L of 10 mM HCl and eluted with 25 mM HCl, and the eluant was monitored for alkaline labile phosphate. The volume of the product (~300 mL) was reduced to ~50 mL by rotary evaporation, the pH adjusted to 3 with KOH, the volume reduced further to 5 mL, and the product stored at -15 °C. Typically, the yield was 70%, and the product contained between 5% and 10% inorganic phosphate, 0.5% DHAP, and 0.075% DGAP.

The  $\text{pK}_a$  values for D,L-GAP and DHAP at 37 °C and ionic strength of 1.0 (KCl) were determined by titration.

**Elimination Reaction of [<sup>32</sup>P]DHAP and [<sup>32</sup>P]LGAP.** Reaction mixtures at ionic strength of 1.0 (KCl) and in a volume of 1.0 mL were incubated for at least 20 min at 37 ± 1 °C, and then the reaction was initiated by the addition of ~10<sup>6</sup> cpm of [<sup>32</sup>P]DHAP or [<sup>32</sup>P]LGAP in a volume of 1 to 20  $\mu\text{L}$  (~1 nmol/ $\mu\text{L}$ ). At specified times 40  $\mu\text{L}$  was withdrawn and diluted into 0.96 mL of a solution containing 100  $\mu\text{L}$  of 4 N H<sub>2</sub>SO<sub>4</sub> and 40  $\mu\text{L}$  of 5% sodium molybdate. Phosphate was extracted as the molybdate complex<sup>9</sup> into 2.0 mL of isobutyl alcohol and unreacted substrate was determined as the counts remaining in the water layer. Values of  $k_{\text{obsd}}$  for the elimination reaction were determined from the slopes of plots of six or more values of  $\ln(C_i - C_\infty)$  against time, where  $C_i$  is counts remaining in the water layer at a given time and  $C_\infty$  is the counts in the water layer at infinite time. The reactions were usually followed for 2 to 3 halftimes and no evidence of curvature in the first-order plots was ever observed. In one case the elimination reaction of D,L-GAP in 0.20 M triethanolamine-HCl (pH 8.1) and ionic strength of 1.0 (KCl) was monitored for inorganic phosphate formation by a colorimetric method.<sup>8</sup> The rate constant obtained by this method was the same as the rate constant obtained for reaction of radiolabeled substrate.

The pH values were determined at the end of the reaction and were constant with increasing buffer concentration except for trifluoroethanol. Second-order rate constants  $k_B$  for general base catalysis were obtained from the slopes of plots of  $k_{\text{obsd}}$  against the concentration of the basic form of the buffer, except for catalysis by trifluoroethoxide, where  $(k_{\text{obsd}} - k_{\text{OH}}[\text{OH}^-])$  was plotted in place of  $k_{\text{obsd}}$  and the concentration of trifluoroethoxide was corrected for the changing pH values.

The slopes and intercepts of all lines were determined by the method of least squares. The first-order and second-order rate constants were reproducible to ±10%.

The products of the elimination reaction of GAP were previously identified as methylglyoxal and phosphate.<sup>2</sup>

**Isomerization and Racemization Reactions of LGAP.** The isomerization reaction of LGAP was followed by coupling the formation of DHAP to the oxidation of NADH with use of  $\alpha$ -glycerolphosphate dehydrogenase.<sup>1</sup> LGAP was adjusted from pH 3 to 7 with KOH, and used immediately after neutralization.<sup>10</sup> Reactions were at an ionic strength

(6) Using the procedure given in the 1982 Calbiochem catalogue.

(7) Glynn, I. M.; Chappell, J. B. *Biochem. J.* **1964**, *90*, 147.

(8) Rose, Z. B.; Pizer, L. I. *J. Biol. Chem.* **1968**, *243*, 4806.

(9) Berenblum, I.; Chain, E. *Biochem. J.* **1938**, *32*, 295.

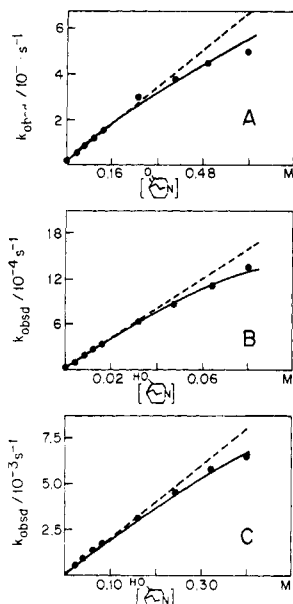


**Figure 2.** Buffer catalysis plots for the elimination reaction of DHAP at 37 °C and ionic strength of 1.0 (KCl): (A) 3-quinuclidinone catalysis,  $[B]/[BH] = 4$ , pH 8.1; (B) 3-quinuclidinol catalysis,  $[B]/[BH] = 1/9$ , pH 9.1; (C) 3-quinuclidinol catalysis,  $[B]/[BH] = 1$ , pH 10.0.

of 1.0 (KCl),  $37 \pm 1$  °C, and were initiated by the addition of LGAP (10–50  $\mu$ L of a 0.2 M solution at pH 7), NADH (enough of a 0.1 M solution to give a final absorbance of  $\sim 0.6$  at 340 nm), and 10  $\mu$ L (5 mg/mL) of  $\alpha$ -glycerolphosphate dehydrogenase. The initial velocity of NADH oxidation was determined for the first 3–10 min of reaction and  $k_{iso}$  values calculated from eq 2 ( $[LGAP]_0$  is the initial concentration of

$$k_{iso} = (d[NADH]/dt)/[LGAP]_0 \quad (2)$$

LGAP). In control experiments it was shown that there was no oxidation of NADH in the absence of LGAP and that the initial velocity of NADH oxidation was unchanged for a 2-fold increase in the concentration of  $\alpha$ -glycerolphosphate dehydrogenase and was directly proportional to the initial concentration of LGAP. Values of  $k_{iso}$  were reproducible to  $\pm 10\%$ .

The combined isomerization and racemization reactions of LGAP were followed by coupling the formation of DHAP and DGAP to NADH oxidation with triosephosphate isomerase and  $\alpha$ -glycerolphosphate dehydrogenase. Under these conditions the left side of eq 2 is the sum of the rate constants for LGAP isomerization and racemization,  $k_{iso} + k_{rac}$ .

## Results

The pH rate profiles for the elimination of phosphate from LGAP and DHAP are shown in Figure 1. The observed rate constants for the reaction of LGAP (upper curve, Figure 1) have been fit to eq 3 where  $k_0 = 8.5 \times 10^{-5} \text{ s}^{-1}$ ,  $k_{OH^-} = 0.24 \text{ M}^{-1} \text{ s}^{-1}$ ,

$$k_{obsd} = \frac{k_0 + k_{OH^-}[OH^-]}{1 + [H^+]/K_1 + K_2/[H^+]} \quad (3)$$

$K_1 = 10^{-5.9} \text{ M}$ , and  $K_2 = 10^{-13} \text{ M}$ . The ionization processes for the equilibrium constants  $K_1$  and  $K_2$  are given in the Discussion. The data for DHAP (lower curve, Figure 1) are less extensive, but it is sufficient to define a pH-independent rate constant  $k_0 = 1.4 \times 10^{-5} \text{ s}^{-1}$  over pH 7–9 and a second-order rate constant  $k_{OH^-} = 0.18 \text{ M}^{-1} \text{ s}^{-1}$  at 0.01–0.05 M  $[OH^-]$ .

Figure 2 shows the dependence of  $k_{obsd}$  for the DHAP elimination reaction on the concentration of the basic buffer form for catalysis by 3-quinuclidinone ( $B/BH = 4$ ) and by 3-quinuclidinol ( $B/BH = 1/9, 1$ ). The plots are linear at low base concentrations and show downward curvature at higher base concentrations. The experimental points are fit to the stepwise elimination reaction mechanism given in the Discussion. Similar curvature is observed in the buffer catalysis plots for LGAP elimination (data not shown).

(10) An increased rate and a nonlinear time course for NADH oxidation were observed with LGAP samples which had been neutralized, frozen, and rethawed.

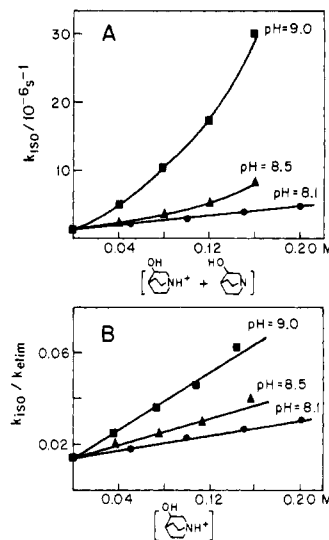


**Figure 3.** Buffer catalysis plots for the isomerization reaction of LGAP at 37 °C, 0.2 M triethanolamine, and ionic strength of 1.0 (KCl): (A) a plot of the rate constants for LGAP isomerization against the total concentration of quinuclidinol buffer at pH 9.0, 8.5, and 8.1; (B) a plot of the ratio of the rate constants for LGAP isomerization and elimination,  $k_{iso}/k_{elim}$ , against the concentration of 3-quinuclidinol cation for reaction at pH 9.0, 8.5, and 8.1.

Table I lists  $k_B$  values for general base catalysis of the DHAP and LGAP elimination reactions, calculated from the slopes of plots of  $k_{obsd}$  against the concentration of the basic form of the buffer over concentrations where the plots are linear. The  $k_B$  values in Table I are independent of the fraction of the buffer in the basic form, showing that general acid catalysis is not significant.

General base catalysis of the elimination reaction of LGAP disappears as the buffer  $pK_a$  is decreased to 7, so that specific salt and medium effects may be estimated from the effects of buffers with low  $pK_a$  on  $k_{obsd}$ . The observed LGAP elimination rate constants are invariant through 0.5 M imidazole buffer concentration at pH 8.2 and decrease 20% through 0.5 M imidazole at pH 6.7. The magnitude of these effects is small relative to catalysis of elimination by all buffers in Table I except triethanolamine catalysis of LGAP elimination, and it is concluded that the contributions of specific salt and medium effects to all other  $k_B$  values in Table I are minimal.

The  $pK_a$  values at 1.0 M KCl and 37 °C for protonation of D,L-GAP and DHAP phosphate dianions are 5.9 and 5.6, respectively. These are 0.4 units lower than the values at 30 °C and 0.1 M NaCl.<sup>11</sup>

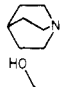
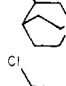
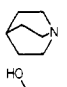
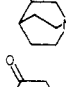
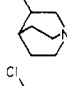
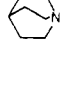
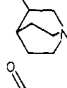
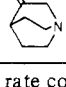
The elimination reaction of DHAP is catalyzed by 3-quinuclidinone at pH 4.9, where the substrate 3-phosphate is predominately in the monoanion form. This is general base catalysis since at the same pH the reaction is not catalyzed by acetate buffers; acetic acid is a 600 times stronger acid than quinuclidinium cation. A  $k_B$  value of  $3.6 \times 10^{-3} \text{ M}^{-1} \text{ s}^{-1}$  for 3-quinuclidinone catalysis of the elimination reaction of DHAP phosphate monoanion is calculated from the observed  $k_B$  at pH 4.9, with a 10% correction for the slower reaction of the phosphate dianion substrate form.

Figure 3A shows the dependence of the observed rate constants for the isomerization of LGAP to DHAP,  $k_{iso}$ , on the total concentration of quinuclidinol buffer. The data in Figure 3A are linearized in Figure 3B by dividing  $k_{iso}$  by the elimination rate constant  $k_{elim}$  at the same buffer concentration ( $k_{elim}$  is measured with radiolabeled substrate as described above) and plotting the rate constant ratio  $k_{iso}/k_{elim}$  against the concentration of the acidic form of the buffer. The data in Figure 3B are fit to eq 4 where

$$k_{iso}/k_{elim} = k_{-0}/k_e + k_{BH}[BH]/k_e \quad (4)$$

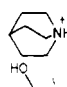
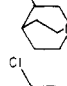
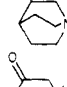
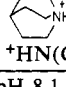
(11) Plaut, B.; Knowles, J. R. *Biochem. J.* **1972**, *129*, 311.

**Table I.** Base Catalysis of the Elimination Reaction of L-Glyceraldehyde 3-Phosphate and Dihydroxyacetone Phosphate Dianions at 37 °C and Ionic Strength of 1.0 (KCl)

LGAP; $k_0 = 8.5 \times 10^{-5} \text{ s}^{-1}$ <sup>a</sup>				DHAP; $k_0 = 1.4 \times 10^{-5} \text{ s}^{-1}$ <sup>a</sup>			
catalyst	pK <sub>a</sub>	f <sub>B</sub>	$k_B/10^{-4} \text{ M}^{-1} \text{ s}^{-1}$ <sup>b</sup>	catalyst	pK <sub>a</sub>	f <sub>B</sub>	$k_B/10^{-4} \text{ M}^{-1} \text{ s}^{-1}$ <sup>b</sup>
OH <sup>-</sup>	15.7		2400	OH <sup>-</sup>	15.7		1800
CF <sub>3</sub> CH <sub>2</sub> O <sup>-</sup>	12.4 <sup>c</sup>	0.50 0.10	610 560	CF <sub>3</sub> CH <sub>2</sub> O <sup>-</sup>	12.4 <sup>c</sup>	0.50 0.10	300 340
N(CH <sub>2</sub> CH <sub>3</sub> ) <sub>3</sub>	11.2 <sup>d</sup>	0.67 0.50	80 104	N(CH <sub>2</sub> CH <sub>2</sub> OH) <sub>3</sub>	8.1 <sup>d</sup>	0.90 0.50	1.5 1.6
CO <sub>3</sub> <sup>2-</sup>	9.9 <sup>d</sup>	0.90 0.75 0.50	21 23 20		11.45 <sup>e</sup>	0.50	905
N(CH <sub>2</sub> CH <sub>2</sub> OH) <sub>3</sub>	8.1 <sup>d</sup>	0.90 0.50	0.7 ~0.5		10.0 <sup>e</sup>	0.50 0.10	185 204
	11.45 <sup>e</sup>	0.50 0.074	1090 1010		9.0 <sup>e</sup>	0.11	71
	10.0 <sup>e</sup>	0.75 0.50 0.25	270 260 290		7.5 <sup>e</sup>	0.44 0.50 0.80	12 11 10
	9.0 <sup>e</sup>	0.50 0.11	84 87				
	7.5 <sup>e</sup>	0.44 0.50 0.80	18 17 18				

<sup>a</sup> The rate constant for the uncatalyzed, pH-independent elimination reaction. <sup>b</sup> The slope of a plot of five or more values of  $k_{\text{obsd}}$  against the concentration of the basic buffer form. <sup>c</sup> Jencks, W. P.; Regenstein, J. In "Handbook of Biochemistry and Molecular Biology, Physical and Chemical Data"; 3rd ed.; Fasman, G. D., Ed.; CRC Press: Cleveland, 1976; Vol. 1, pp 305-351. <sup>d</sup> Calculated from the observed pH and the acid:base buffer ratio. <sup>e</sup> pK<sub>a</sub> values determined at 25 °C and ionic strength of 1.0 (KCl) Gresser, M. J.; Jencks, W. P. *J. Am. Chem. Soc.* 1977, 99, 6963. The pK<sub>a</sub> values at 37 °C calculated from the observed pH and the acid:base buffer ratio differed by <0.1 unit from the pK<sub>a</sub> at 25 °C.

**Table II.** Rate Constant Ratios for Partitioning of Enediolate between Buffer-Catalyzed Protonation and Uncatalyzed Leaving Group Expulsion<sup>a</sup>

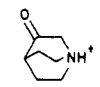
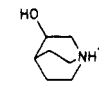
catalyst	pK <sub>a</sub>	$k_{\text{BH}}/k_e (\text{M}^{-1})^d$
	11.45 <sup>b</sup>	0.021
	10.0 <sup>b</sup>	0.077 ± 0.05 <sup>e</sup>
	9.0 <sup>b</sup>	0.27
	7.5 <sup>b</sup>	1.4
<sup>+</sup> HN(C <sub>2</sub> H <sub>4</sub> OH) <sub>3</sub>	8.1 <sup>c</sup>	0.048 ± 0.08 <sup>e</sup>

<sup>a</sup> At pH 8.1 and ionic strength of 1.0 (KCl). Solutions containing 3-substituted quinuclidines were buffered with 0.2 M triethanolamine. <sup>b</sup> pK<sub>a</sub> values determined at 25 °C and ionic strength of 1.0 (KCl) (Gresser, M. J.; Jencks, W. P. *J. Am. Chem. Soc.* 1977, 99, 6963). The pK<sub>a</sub> values at 37 °C calculated from the observed pH and the acid:base buffer ratio differed by <0.1 units from the pK<sub>a</sub> at 25 °C. <sup>c</sup> Calculated from the observed pH and BH/B ratios. <sup>d</sup> The slope of a plot of five values of  $k_{\text{iso}}/k_{\text{elim}}$  against the concentration of the acidic buffer form. <sup>e</sup> Average of values obtained in two different experiments.

$k_{\text{BH}}/k_e$  and  $k_{-0}/k_e$  are the slopes and intercepts respectively of the lines in Figure 3B. In the discussion it will be shown that the rate constant ratios in eq 4 are for partitioning of the enediolate intermediate between protonation ( $k_{-0}$  and  $k_{\text{BH}}$ ) and leaving group expulsion ( $k_e$ ).

The rate constant ratios  $k_{\text{BH}}/k_e$  at pH 8.1 for a number of different catalysts are listed in Table II. Table III list values

**Table III.** Rate Constant Ratios for Partitioning of Enediolate between Protonation and Elimination at Different pH Values<sup>a</sup>

pH	catalyst		
	none $k_{-0}/k_e^b$	 $k_{\text{BH}}/k_e (\text{M}^{-1})^c$	 $k_{\text{BH}}/k_e (\text{M}^{-1})^c$
6.2 <sup>d</sup>		0.089	
6.4 <sup>d</sup>			≤0.005 <sup>g</sup>
6.6 <sup>d</sup>	0.010	0.11	
7.1 <sup>e</sup>		0.24	
7.3 <sup>e</sup>	0.0086		
7.4 <sup>e</sup>		0.29	
7.5 <sup>e</sup>		0.34 ± 0.03 <sup>f</sup>	0.038
8.1 <sup>e</sup>	0.007	1.4	0.077 ± 0.05 <sup>f</sup>
8.5 <sup>e</sup>		2.5	0.16
9.0 <sup>e</sup>	0.009		0.30
10			0.40 <sup>h</sup>

<sup>a</sup> At 37 °C and ionic strength of 1.0 (KCl). <sup>b</sup>  $k_{\text{iso}}/k_{\text{elim}}$  extrapolated to zero concentration of imidazole or triethanolamine buffer. <sup>c</sup> The slope of a plot of five values of  $k_{\text{iso}}/k_{\text{elim}}$  against the concentration of the acidic buffer form. <sup>d</sup> Imidazole buffer (0.2 M). <sup>e</sup> Triethanolamine buffer (0.2 M). <sup>f</sup> Average of values obtained in two different experiments. <sup>g</sup> Limit calculated assuming a 20% increase in  $k_{\text{iso}}$  could have been detected at 0.8 M quinuclidinium ion. <sup>h</sup> Value calculated from data in Figure 2C (see text).

at different pHs for the rate constant ratio  $k_{-0}/k_e$  and the ratios  $k_{\text{BH}}/k_e$  for 3-quinuclidinol and 3-quinuclidinol cations. The specific KCl salt effect on  $k_{\text{iso}}$  is small;  $k_{\text{iso}}$  for reaction at pH 8.1 in 0.1 M triethanolamine increases from  $8.1 \times 10^{-7} \text{ s}^{-1}$  at 0.9 M KCl to  $11.4 \times 10^{-7} \text{ s}^{-1}$  at zero KCl.

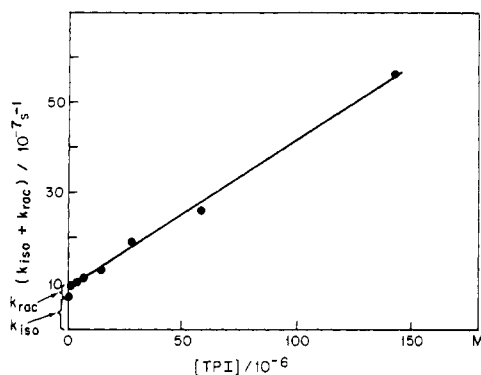


**Figure 4.** The dependence of  $k_{\text{iso}} + k_{\text{rac}}$  on triose phosphate isomerase concentration for reaction of LGAP at 37 °C, pH 7.0 (0.1 M triethanolamine), and ionic strength of 1.0 (KCl). The LGAP concentration was 8 mM.

Figure 4 shows the dependence of the sum of the rate constants for LGAP isomerization and racemization,  $k_{\text{iso}} + k_{\text{rac}}$ , on triose phosphate isomerase concentration at pH 7.0 (0.1 M triethanolamine-HCl), ionic strength of 1.0 (KCl) and  $[\text{LGAP}]_0 = 8$  mM. The value of the intercept of this plot ( $8.6 \times 10^{-7} \text{ s}^{-1}$ ) is slightly greater than the  $k_{\text{iso}}$  value observed in the absence of triose phosphate isomerase ( $7.1 \times 10^{-7} \text{ s}^{-1}$ ).

There is a large solvent deuterium isotope effect on  $k_{\text{iso}}$ . The  $k_{\text{BD}}/k_{\text{e}}$  value for catalysis by 3-quinuclidinol cation ( $\text{B}/\text{BD} = 0.77$ ) is  $0.091 \text{ M}^{-1}$  in  $\text{D}_2\text{O}$ , and the value in  $\text{H}_2\text{O}$  at the same buffer ratio (pH 7.4 value in Table III) is  $0.29 \text{ M}^{-1}$ .

The rate constants for 3-quinuclidinol catalysis of LGAP and DHAP elimination ( $\text{B}/\text{BD} = 0.77$ ) in  $\text{D}_2\text{O}$  are  $1.7 \times 10^{-3}$  and  $1.1 \times 10^{-3} \text{ M}^{-1} \text{ s}^{-1}$ , respectively. Buffer curvature for quinuclidinol catalysis of DHAP elimination is less pronounced in  $\text{D}_2\text{O}$  than in  $\text{H}_2\text{O}$ ; in  $\text{H}_2\text{O}$  the buffer catalysis plot is similar to the plots in Figure 2 and the  $k_{\text{obsd}}$  value at 0.9 M total buffer concentration deviates by 20% from the line through  $k_{\text{obsd}}$  values at lower buffer concentrations, while in  $\text{D}_2\text{O}$  there is a much better fit of all the points to a single line and only a 9% deviation at 0.9 M total buffer concentration (data not shown).

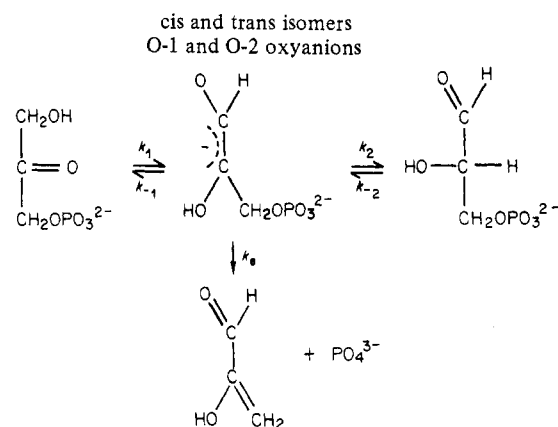
## Discussion

**Enediolate Intermediate.** Rose and Iyengar<sup>3</sup> have proposed that the nonenzymatic isomerization and elimination reactions of GAP and DHAP proceed through a common enediolate intermediate (Scheme I). This is a priori the expected mechanism by analogy with halogenation of positions  $\alpha$  to a carbonyl group<sup>12,13</sup> and E1cB elimination reactions,<sup>14</sup> both of which proceed through enolate intermediates. In addition there is no precedent for a concerted elimination reaction when the enolate is stable enough to exist in water.<sup>15</sup> Further support that isomerization and elimination are through an enediolate intermediate is provided by the following experimental observations.

1. The elimination reaction of DHAP must be through the enediolate intermediate (O-1 oxyanion) because the direct elimination of phosphate at a carbon  $\alpha$  to the carbonyl group is slow; the deoxy analogue of DHAP is stable for 10 h at room temperature in 0.1 M NaOH,<sup>16,17</sup> conditions which would degrade DHAP with a half-time of about 2 min. Hydrogen migration from O-1 to O-2 at the enolate formed from C-3 DHAP deprotonation gives the same intermediate as is formed from GAP deprotonation.

2. The similarity in the rate constants for hydroxide-catalyzed elimination of DHAP ( $0.56 \text{ M}^{-1} \text{ s}^{-1}$ )<sup>18</sup> and hydroxide-catalyzed

## Scheme I



deprotonation of acetone ( $0.25 \text{ M}^{-1} \text{ s}^{-1}$  at 25 °C and ionic strength of 0.2)<sup>19</sup> is evidence that DHAP deprotonation at C-3 is the rate-determining step for DHAP elimination and that the enediolate is an intermediate of this reaction.

3. The rate constants for hydroxide catalysis of the  $\beta$ -elimination reactions of LGAP ( $5.6 \text{ M}^{-1} \text{ s}^{-1}$ )<sup>18</sup> and 4-(4-nitrophenoxy)-2-oxobutane-1 phosphate ( $2.1 \text{ M}^{-1} \text{ s}^{-1}$  at 25 °C and ionic strength of 1.0, KCl)<sup>20</sup> are similar. This is inconsistent with a concerted elimination reaction mechanism in which there is substantial cleavage of the bond to the leaving group in the reaction transition state because for this mechanism the rate constant will depend on the basicity of the leaving group and a smaller rate constant is expected for the elimination of the more basic phosphate trianion from LGAP dianion.

4. The second-order dependence of the observed LGAP isomerization rate constant  $k_{\text{iso}}$  on total buffer concentration (Figure 3A) is consistent with first-order catalysis of substrate deprotonation by the basic form of the buffer and first-order catalysis of enediolate protonation by the acidic form of the buffer. General base catalysis of substrate deprotonation increases the steady-state enediolate concentration, and general acid catalysis of enediolate protonation diverts the enediolate reaction from elimination to isomerization because leaving group expulsion ( $k_{\text{e}}$ , Scheme I) is not expected to be general acid catalyzed.<sup>14b,d,21</sup>

5. The different solvent isotope effects on the quinuclidinol-catalyzed elimination reaction of LGAP,  $(k_{\text{B}})_{\text{H}_2\text{O}}/(k_{\text{B}})_{\text{D}_2\text{O}} = 1.1$ , and on the quinuclidinol-catalyzed isomerization reaction of LGAP,  $(k_{\text{BH}}/k_{\text{e}})_{\text{H}_2\text{O}}/(k_{\text{BD}}/k_{\text{e}})_{\text{D}_2\text{O}} = 3.2$ , are consistent with a two-step mechanism and a common enediolate intermediate; deprotonation of the hydrogen-labeled substrate ( $k_{-2}$ ) is the rate-determining step for elimination, while the general acid catalyzed isomerization reaction is sensitive to the primary kinetic isotope effect on the rate constant for enediolate protonation by quinuclidinol cation ( $k_{-1}$ ).

6. Plots of  $k_{\text{obsd}}$  against buffer concentration for the elimination reaction of DHAP bend downward at high 3-quinuclidinol and 3-quinuclidinol buffer concentrations (Figure 2). There are a large number of possible explanations for this curvature,<sup>22</sup> one of which is a partial change in rate-determining step from buffer catalyzed, rate-determining substrate deprotonation ( $k_1$ ) at low buffer concentrations to uncatalyzed, rate-determining leaving group expulsion ( $k_{\text{e}}$ ) at high buffer concentrations. This interpretation is supported by experimentally determined rate constant ratios for enediolate partitioning between elimination and buffer-catalyzed protonation: at high buffer concentrations the rate

(12) Lapworth, A. *J. Chem. Soc.* **1904**, 30.

(13) Jones, J. R. "The Ionization of Carbon Acids"; Academic Press: London, 1973.

(14) (a) Fedor, L. R. *J. Am. Chem. Soc.* **1967**, *89*, 4479. (b) Fedor, L. R. *Ibid.* **1969**, *91*, 908. (c) Cavestri, R. C.; Fedor, L. R. *Ibid.* **1970**, *92*, 4610. (d) Fedor, L. R.; Glave, W. R. *Ibid.* **1971**, *93*, 985.

(15) (a) Jencks, W. P. *Chem. Soc. Rev.* **1981**, *10*, 345. (b) Jencks, W. P. *Acc. Chem. Res.* **1980**, *13*, 161.

(16) Putnam, S. J.; Coulson, A. F. W.; Farley, I. R. T.; Riddleston, B.; Knowles, J. R. *Biochem. J.* **1972**, *129*, 301.

(17) Rose, I. A.; O'Connell, E. L. *J. Biol. Chem.* **1969**, *244*, 126.

(18) The observed  $k_{\text{OH}^-}$  value from Table I corrected for the presence of 68% DHAP<sup>23</sup> or 95.7% LGAP<sup>24</sup> in the unreactive hydrated form.

(19) Bell, R. P. "The Proton in Chemistry"; 2nd ed.; Cornell University Press: Ithaca, New York, 1973; p 150.

(20) (a) Wilde, J.; Hunt, W.; Hupe, D. J. *J. Am. Chem. Soc.* **1977**, *99*, 8319. (b) Motiu-DeGrood, R.; Hunt, W.; Wilde, J.; Hupe, D. J. *J. Am. Chem. Soc.* **1979**, *101*, 2182.

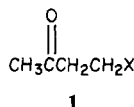
(21) Keefe, J. R.; Jencks, W. P. *J. Am. Chem. Soc.* **1983**, *105*, 265.

(22) Hand, E. S.; Jencks, W. P. *J. Am. Chem. Soc.* **1975**, *97*, 6221.

constant  $k_{\text{BH}}[\text{BH}]$  for enediolate protonation at C-1 approaches  $k_e$ , as required for a change in rate-determining step (see discussion of isomerization reaction).

**Elimination Reactions of DHAP and LGAP.** Evidence for a common enediolate intermediate in the elimination reactions of DHAP and GAP was presented above. The observed general base catalysis is evidence for rate-determining deprotonation and an Elcb irreversible mechanism ( $k_e \gg k_{-1}$ ,  $k_2$ , Scheme I) because carbon deprotonation is strongly catalyzed by general bases,<sup>13</sup> while leaving group expulsion from a carbanion intermediate is usually not buffer catalyzed.<sup>14b,d,21</sup> At low buffer concentrations the observed rate constants for elimination are the same as the rate constants for substrate deprotonation, because virtually every substrate deprotonation gives elimination products.

The elimination reactions of DHAP and GAP resemble the  $\beta$ -elimination reactions of a series of 4-substituted-2-oxobutanes (1) studied by Fedor.<sup>14</sup> These substrates were shown to react



through an enolate intermediate which was reversibly protonated when the leaving group was methoxide<sup>14b</sup> and which expelled the less basic acetate and benzoate leaving groups at a much faster rate than reprotonation.<sup>14a,c</sup> For triose phosphates the leaving group is either the phosphate dianion or trianion, and the elimination reaction is always Elcb irreversible except at high concentrations of substituted quinuclidinone buffers where curvature in the buffer catalysis plots (Figure 2) suggests a change in rate-determining step. The partitioning of the enediolate between phosphate expulsion and reprotonation will depend on the ionization state of the phosphate leaving group, and our results are consistent with  $k_e \gg k_{-1}$ ,  $k_2$  (Scheme I) for partitioning of the enediolate phosphate monoanion, and approximately equal rates of leaving group expulsion and enediolate reprotonation for partitioning of the enediolate phosphate dianion at high buffer concentrations. This interpretation is supported by studies of the isomerization reaction (see the following section).

It is useful to correct the observed elimination constants for the fraction of hydrated DHAP or LGAP, because these substrate forms are expected to be unreactive. Rate constants for reaction of the carbonyl form of DHAP and GAP can be obtained by dividing the observed rate constants by the fraction of the carbonyl substrate: 0.32 and 0.043 respectively for DHAP<sup>23</sup> (at 37 °C) and GAP<sup>24</sup> (at 40 °C). The corrected rate constants for LGAP elimination are larger than those for DHAP elimination; i.e., the position  $\alpha$  to the aldehyde group is about 10 times more reactive for deprotonation than the position  $\alpha$  to the keto group.

The elimination reaction of LGAP is hydroxide catalyzed between pH 10 and 13 (Figure 1). At very high pH there is a downward break in the pH rate profile which may be due to a decrease in the concentration of the active aldehyde form of the substrate caused by ionization of the aldehyde hydrate of LGAP. The data in Figure 1 are also fit by eq 5, which is derived with

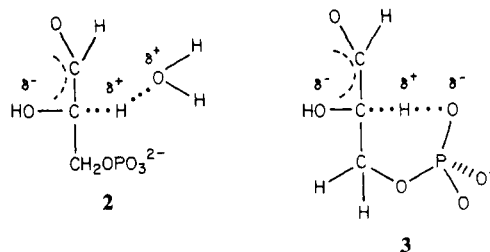
$$k_{\text{obsd}} = \frac{1}{K_{\text{H}}} \left( \frac{k'_0 + k'_{\text{OH}}[\text{OH}^-]}{1 + [\text{H}^+]/K_1 + K_2/[\text{H}^+]} \right) \quad (5)$$

the assumptions that only the carbonyl form of LGAP undergoes elimination and that  $(1 + K_{\text{H}}) \sim K_{\text{H}}$  ( $K_{\text{H}} = 22$  is the equilibrium constant for LGAP phosphate dianion and monoanion hydration).<sup>24</sup> The primed rate constants in eq 5 are for reaction of the carbonyl substrate form. The downward break at high pH is fit by  $K_2 = 10^{-13}$  M in both eq 3 and 5. This is similar to the value of  $10^{-13.3}$  M for formaldehyde hydrate ionization.<sup>25</sup>

At high pH the rate constant for LGAP elimination approaches the rate constant for the uncatalyzed hydration of LGAP<sup>24</sup> and the downward break at pH 13 could be attributed to a change from rate-determining deprotonation to rate-determining dehydration. This is ruled out because the hydration reaction will also be strongly catalyzed by hydroxide.<sup>26,27</sup> Similarly dehydration can never be rate determining at high buffer concentrations<sup>28</sup> since in all cases but quinuclidine the uncatalyzed hydration rate is much faster than buffer-catalyzed elimination, and in the case of the exception the hydration rate is expected to be increased substantially by buffer catalysis.<sup>26-28</sup>

At pH lower than 10 the rate constant for the pH-independent reaction of LGAP or DHAP,  $k_0$ , is larger than  $k_{\text{OH}}[\text{OH}^-]$  and the observed elimination rate constants are pH independent. The pH rate profile (Figure 1) shows a downward break centered at pH 6 which is fit by the titrimetric  $\text{p}K_{\text{a}}$  of 5.9 ( $K_1$ , eq 3) for protonation of LGAP phosphate dianion. This suggests that the protonated species has a greatly reduced elimination rate constant. The downward break for DHAP reaction occurs at a lower pH than for LGAP reaction as expected since the  $\text{p}K_{\text{a}}$  for DHAP is 0.3 units smaller than that for LGAP.

There are two kinetically equivalent transition states for the pH-independent reaction of LGAP and DHAP phosphate dianions: **2** (water-catalyzed deprotonation) and **3** (intramolecular deprotonation by phosphate dianion). The following observations establish that **3** is the reaction transition state.



1. DHAP and acetone are deprotonated by hydroxide at similar rates, but the rate constant for pH-independent DHAP deprotonation is  $10^5$  times larger than the rate constant for acetone deprotonation by water.<sup>29</sup> This shows that the phosphate dianion specifically accelerates the rate of pH-independent C-3 deprotonation.

2. If water is acting as a base then the deprotonation of DHAP phosphate monoanion by water must be much slower than dianion deprotonation in order to account for the downward break in the pH rate profile. This is unlikely because 3-quinuclidinone deprotonation of DHAP phosphate monoanion is slightly faster (3-fold) than DHAP phosphate dianion deprotonation.<sup>30</sup>

3. General base catalysis of the elimination reaction is observed only for bases with a  $\text{p}K_{\text{a}}$  higher than that for LGAP phosphate dianion, because only these bases are reactive enough to deprotonate triose phosphates faster than intramolecular phosphate dianion deprotonation.

Intramolecular deprotonation by phosphate dianion has been previously reported for the elimination reaction of 4-(4-nitro-phenoxy)-2-oxobutane-1 phosphate,<sup>20</sup> and intramolecular carboxylate and amine deprotonation have been reported for the reaction of a series of  $\omega$ -carboxy-substituted 2-ketones<sup>31a</sup> and  $\omega$ -amino-substituted 2-ketones,<sup>31b</sup> respectively.

The Brønsted plots for general base catalysis of the elimination reaction of LGAP and DHAP are shown in Figure 5. A rate

(26) Funderburk, L. H.; Aldwin, L.; Jencks, W. P. *J. Am. Chem. Soc.* **1978**, *100*, 5444.

(27) Bell, R. P.; Evans, P. G. *Proc. R. Soc. London, Ser. A* **1966**, *291*, 297.

(28) Emly, M.; Leussing, D. L. *J. Am. Chem. Soc.* **1981**, *103*, 628.

(29) The value for water-catalyzed deprotonation of acetone at 25 °C and ionic strength of 0.2 is  $4.6 \times 10^{-10} \text{ s}^{-1}$ .<sup>19</sup>

(30) General acid catalysis is not the expected mechanism for quinuclidinone buffer catalyzed deprotonation of DHAP at pH 4.9 because no catalysis is observed for acetic acid which is a considerably stronger acid.

(31) (a) Bell, R. P.; Fluendy, A. D. *Trans. Faraday Soc.* **1963**, *59*, 1623.

(b) Coward, J. K.; Bruice, T. C. *J. Am. Chem. Soc.* **1969**, *91*, 5339.

(23) Reynolds, S. J.; Yates, D. W.; Pogson, C. I. *Biochem. J.* **1971**, *122*, 285.

(24) Trentham, D. R.; McMurray, C. H.; Pogson, C. I. *Biochem. J.* **1969**, *114*, 19.

(25) Bell, R. P.; Onwood, D. P. *Trans. Faraday Soc.* **1962**, *58*, 1557.

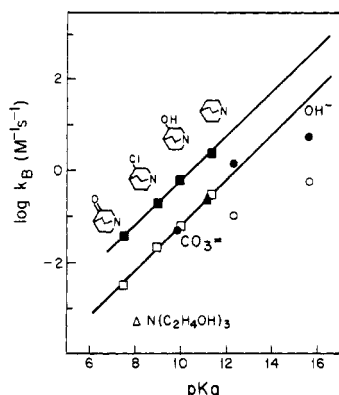


**Figure 5.** The Brønsted plots for general base catalysis of LGAP phosphate dianion elimination (closed symbols) and DHAP phosphate dianion elimination (open symbols). The rate constants are those observed for buffer catalysis (Table I), corrected for the fraction of the substrate in the unreactive hydrated form (95.7% and 68% respectively for LGAP<sup>24</sup> and DHAP<sup>23</sup>): squares, 3-substituted quinuclidines; circles, anionic bases; triangles, trialkylamines.

constant of  $3.8 \times 10^{-5} \text{ M}^{-1} \text{ s}^{-1}$  for intermolecular LGAP deprotonation by LGAP phosphate dianion is estimated by extrapolating the line through substituted quinuclidines to  $\text{p}K_a$  6 and assuming that the dianionic phosphate base shows the same 1 log unit negative deviation as carbonate. Combining this value with  $k_0$  (Table I) gives an effective molarity of 2.3 for the intramolecular reaction; i.e., the phosphate dianion of GAP is 2.3 times more reactive in the intramolecular reaction than 1 M of a base with the same  $\text{p}K_a$  in an intermolecular reaction. The effective molarity for the reaction of DHAP is 0.7. The larger effective molarity for LGAP than DHAP shows that intramolecular carbon deprotonation is more favored for LGAP. The apparent preference of a six-membered over a seven-membered cyclic transition state for intramolecular carbon deprotonation has been noted previously.<sup>31a</sup> The donor-proton-acceptor bonds in six- and seven-membered rings are expected to deviate from the most stable linear configuration. Linearity is more easily achieved in eight- or nine-membered rings so that intramolecular carbon deprotonation through an intervening water molecule<sup>32</sup> is a reasonable, though unestablished, possibility.

The slopes of the Brønsted plots for general base catalysis by 3-substituted quinuclidines (Figure 5) are 0.48 and 0.45 respectively for reaction of DHAP and GAP. Other bases show marked deviation from this plot. The Brønsted  $\beta$  value of 0.48 for DHAP reaction is substantially smaller than the  $\beta$  of 0.88 for acetone deprotonation by four substituted carboxylate anions<sup>33</sup> and the  $\beta$  value of 0.75 for base catalysis of the Elcb irreversible elimination reaction of 4-(4-nitrophenoxy)-2-oxobutane by ten anionic bases with  $\text{p}K_a$ s from 4.8 to 10.6.<sup>34</sup> This is a striking example of a change in  $\beta$  which is unrelated to movement of the reaction transition state induced by changing substrate reactivity,<sup>35a</sup> since all three of the above substrates have a similar reactivity with hydroxide. One explanation for the smaller  $\beta$  value for DHAP deprotonation is that the effective charge "seen"<sup>35b</sup> by the buffer catalyst in the reaction transition state is decreased by electrostatic interactions between the buffer and the substrate phosphate dianion.

The deviations from the Brønsted line defined by 3-substituted quinuclidines are due to a number of different factors. We attribute the 13-fold greater  $k_B$  value for quinuclidinol compared to carbonate catalysis (the two buffers have similar  $\text{p}K_a$ s) primarily to a difference in the electrostatic interactions between the buffer and the dianionic substrate which will stabilize the transition state

containing the partially positively charged amine catalyst and destabilize the transition state containing the negatively charged carbonate catalyst. Similar differences in catalytic rate constants for neutral and anionic bases have been observed in related systems.<sup>28,36</sup>

An additional factor contributes to the hydroxide deviation since hydroxide also deviates from Brønsted correlations of the rate constants for carbon deprotonation by anionic bases.<sup>34,37</sup> This deviation has been attributed to an abnormally large desolvation energy for hydroxide and an unbalanced transition state in which desolvation is considerably more advanced than proton transfer.<sup>34,35b,37</sup>

The downward deviation for triethanolamine from the line for 3-substituted quinuclidines may be due to steric hindrance to deprotonation by triethanolamine, which has greater conformational flexibility than quinuclidine; steric hindrance to amine protonation is expected to be greater in the transition state for carbon deprotonation than in the equilibrium amine protonation reaction because in the former the base interacts with the triose phosphate substrate but in the latter only with a proton.

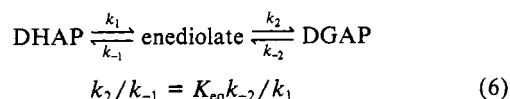
The  $k_B$  value for quinuclidinol catalysis of DHAP phosphate monoanion elimination is 3 times larger than that for dianion elimination. This is consistent with weakened electrostatic interactions between the oxyanion and the phosphate, a lower  $\text{p}K_a$ , and greater stability for the enolate oxyanion when the phosphate is in the monoanionic form; stabilization of the intermediate is expected to be reflected in the transition state for formation of the intermediate and to give an increased  $k_B$  value.

**Isomerization and Racemization of LGAP.** The isomerization reaction of LGAP was studied by the method of Hall and Knowles.<sup>1</sup> Our rate constant for LGAP isomerization at pH 8.1, 0.1 M triethanolamine, and no KCl is  $1.1 \times 10^{-6} \text{ s}^{-1}$ . This is about 4 times smaller than the value of  $4.3 \times 10^{-6} \text{ s}^{-1}$  reported by Hall for isomerization of a D,L-GAP mixture at 30 °C and 0.04 M bicarbonate.<sup>1</sup> The larger value may be due to buffer catalysis by bicarbonate.

We have reported data as the rate constant ratio  $k_{\text{iso}}/k_{\text{elim}}$  where  $k_{\text{iso}}$  and  $k_{\text{elim}}$  are the observed rate constants for isomerization and elimination of LGAP under identical reaction conditions. The product rate constant ratio  $k_{\text{iso}}/k_{\text{elim}}$  is the same as the rate constant ratio for partitioning of the enediolate intermediate between C-1 protonation and leaving group expulsion. The observation that partitioning greatly favors elimination ( $k_{\text{elim}} \gg k_{\text{iso}}$ ) except at high buffer concentrations is consistent with the Elcb irreversible mechanism assigned for the elimination reaction of DHAP.

DGAP formation by enediolate protonation at C-2 was estimated by coupling DGAP formation to NADH oxidation with triose phosphate isomerase (TPI) and  $\alpha$ -glycerolphosphate dehydrogenase. Addition of the lowest concentration of TPI causes a relatively sharp increase in  $k_{\text{iso}}$  +  $k_{\text{rac}}$ , and further additions give a more shallow increase (Figure 4). The difference between the y intercept in Figure 4 and  $k_{\text{iso}}$  observed with no TPI is the rate constant  $k_{\text{rac}}$  for the uncatalyzed racemization of LGAP (buffer catalysis is not important in this experiment). The positive slope of Figure 4 shows that TPI also catalyzes the isomerization and (or) the racemization reactions of LGAP. This corresponds either to enzymatic protonation of the enediolate or to the direct reaction of enzyme with LGAP.

The  $k_{\text{iso}}/k_{\text{elim}}$  and  $k_{\text{rac}}/k_{\text{elim}}$  values for uncatalyzed isomerization and racemization calculated from Figure 4 are 0.0083 and 0.0018, respectively. The experimentally determined ratio of 0.0018/0.0083 = 0.22 for partitioning of the enediolate between C-2 and C-1 protonation is in fair agreement with the ratio of 0.14 calculated from eq 6 with a statistically corrected value of 1/44 for



(32) Gandour, R. D. *Tetrahedron Lett.* **1974**, 295.

(33) Bell, R. P.; Lidwell, O. M. *Proc. R. Soc. London, Ser. A* **1949**, 176, 88.

(34) Hupe, D. J.; Wu, D. *J. Am. Chem. Soc.* **1977**, 99, 7653.

(35) (a) Jencks, D. A.; Jencks, W. P. *J. Am. Chem. Soc.* **1977**, 99, 7948.

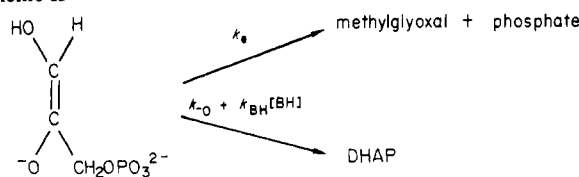
(b) Hupe, D. J.; Jencks, W. P. *Ibid.* **1977**, 99, 451.

(36) Thibblen, A. *J. Am. Chem. Soc.* **1984**, 106, 183.

(37) Jencks, W. P.; Brant, S. R.; Gandler, J. R.; Fendrich, G.; Nakamura, C. *J. Am. Chem. Soc.* **1982**, 104, 7045.



## Scheme II



$K_{eq}^{38}$  (the equilibrium constant for isomerization of DHAP to DGAP) and 6 for  $k_{-2}/k_1$  (the ratio of  $k_0$  values in Table I for the pH-independent elimination reaction of LGAP and DHAP). C-2 protonation of the enediolate by buffer to give DGAP is not experimentally significant because the  $k_{-2}/k_1$  ratio for buffer catalysis of LGAP and DHAP deprotonation is less than 2 (Table I), while the isomerization equilibrium strongly favors the formation of DHAP.<sup>38</sup>

The observed partition ratio of 0.22 for  $k_2/k_{-1}$  differs markedly from values of 3.2<sup>3</sup> and 3.6<sup>1</sup> reported previously. We do not have a good explanation for these different values; however, the ratio which we obtain is internally consistent with other data reported here, since it is in fair agreement with the ratio calculated from the rate and equilibrium constants on the right side of eq 6. The larger partition ratio is inconsistent with our results; this ratio and a rearranged form of eq 6 have been used to calculate a rate constant for DHAP deprotonation ( $3.8 \times 10^{-7} \text{ s}^{-1}$ )<sup>1</sup> which is 40 times smaller than the observed rate constant for uncatalyzed DHAP deprotonation ( $k_0$  in Table I).

Values of  $k_{iso}$  for LGAP isomerization show a second-order dependence on total buffer concentration (Figure 3A). Isomerization with rate-determining formation of an enediol intermediate through a transition state containing two buffer molecules is ruled out because termolecular catalysis of acetone enolization was not previously observed by buffers with  $pK_a > 5$ .<sup>39a</sup> In addition this mechanism cannot account for the observed quinuclidinium catalysis (Table II) since the transition state for general base catalysis of enediolate formation is not expected to be significantly stabilized by a buffer acid with nearly the same  $pK_a$  as the enediolate oxyanion.<sup>39b,40</sup>

The second-order dependence of  $k_{iso}$  on buffer concentration is due to the combined effects of first-order catalysis of substrate deprotonation by buffer base, which increases the rate constant for all reactions through the enediolate intermediate, and first-order catalysis of enediolate protonation by the buffer acid, which increases the fraction of enediolate which partitions to DHAP. Dividing  $k_{iso}$  by  $k_{elim}$  cancels out the effect of the basic buffer form. The slope of the plots in Figure 3B,  $k_{BH}/k_e$  (eq 4), is the ratio of the rate constants for buffer-catalyzed protonation of the enediolate at C-1 and expulsion of phosphate from the enediolate, while the intercept is the rate constant ratio  $k_{-O}/k_e$  (eq 4), where  $k_{-O}$  is the rate constant for the buffer-independent protonation of the enediolate at C-1 (Scheme II). Equation 4 holds because enediolate formation is rate determining for substrate reaction: the ratio of the rate constants for product formation by partitioning of an intermediate after the rate-determining step is equal to the ratio of the rate constants for the reaction of the intermediate along the two pathways. Other examples of this are the  $k_{az}/k_s$  values calculated from product ratios for azide and solvent reaction with the carbocations which are intermediates of the  $S_N1$  reactions of 1-phenylethyl derivatives.<sup>41</sup>

General acid catalysis of leaving group expulsion would require that  $k_{iso}/k_{elim}$  values approach a limiting, buffer-independent value

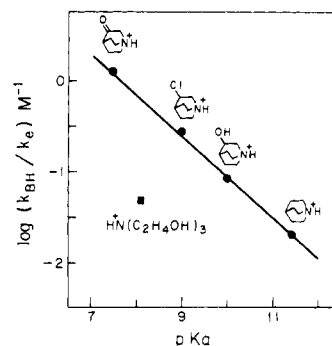


Figure 6. The Brønsted plot for general acid catalysis of enediolate protonation at C-1. Reaction was at 37 °C, ionic strength of 1.0 (KCl), and pH 8.1 (0.2 M triethanolamine).

## Scheme III



at high buffer concentrations, since both pathways for enediolate reaction would contain a term first order in the buffer acid species. There is no evidence for downward curvature at high buffer concentrations in Figure 3B; therefore general acid catalysis of the expulsion of phosphate from the enediolate is minimal, in agreement with past results for related reactions.<sup>14b,d,21</sup>

$\log k_{BH}/k_e$  values for catalysis by several different buffers at pH 8.1 are plotted against the buffer  $pK_a$  in Figure 6. The slope of this plot, 0.47, is equal to the Brønsted  $\alpha$  value for enediolate protonation at C-1. This is the reverse of the deprotonation of DHAP at C-1 which is rate determining for DHAP elimination. The Brønsted plots in Figures 5 and 6 meet two thermodynamic requirements for buffer catalysis of a reaction in the forward and reverse directions.

1. The sum  $\beta + \alpha = 0.95$  is equal, within experimental error, to the thermodynamically required value of 1.00.

2. The deviation of the rate constant for general base catalysis by triethanolamine from the Brønsted plot for general base catalysis by 3-substituted quinuclidines (1.16 log units) is equal within experimental error to the deviation of the rate constant ratio for the triethanolamine cation from the Brønsted plot for the reaction of 3-substituted quinuclidinium ions (1.14 log units).

A good fit of the observed rate constants for buffer catalysis of DHAP elimination (Figures 2A and 2B) is obtained by substitution of the rate constant ratios for enediolate partitioning ( $k_{BH}/k_e$  and  $k_{-O}/k_e$ , Table III) into eq 7 for Scheme III. (The

$$k_{obsd} = (k_0 + k_B[B]) \left( \frac{k_e}{k_{-O} + k_{BH}[BH] + k_e} \right) \quad (7)$$

fit to data in Figure 2B for reaction at pH 9.1 is based on the  $k_{BH}/k_e$  value at pH 9.0. There is only a 33% increase in  $k_{BH}/k_e$  for quinuclidinium protonation for a pH increase from 9 to 10 (Table III). We conclude, therefore, that the buffer curvature observed in Figure 2 is due to a partial change in the rate-determining step for DHAP elimination reaction from substrate deprotonation at low buffer concentration to leaving group expulsion at high buffer concentrations.

The curvature in the buffer-dependence plot for the elimination reaction of DHAP in  $D_2O$  is less pronounced than that in  $H_2O$ . This is consistent with a smaller fraction of enediolate return to DHAP in  $D_2O$  than in  $H_2O$  and is in agreement with the solvent deuterium isotope effect of 3.2 on the ratio  $k_{BH}/k_e$  for quinuclidinium catalysis of the isomerization reaction. The isotope effect on  $k_{BH}/k_e$  is consistent with a large primary isotope effect on  $k_{BH}$ , but the precise magnitude of the isotope effect on  $k_{BH}$  is uncertain because the ratio of the  $k_e$  values in the protium and deuterium solvents is not known. The large solvent deuterium isotope effect on  $k_{BH}$  shows that a solvent-derived proton is used to protonate the enediolate at C-1, so that isomerization with intramolecular proton transfer is not a major reaction.

(38) Veech, R. L.; Raijman, L.; Dalziel, K.; Krebs, H. A. *Biochem. J.* **1969**, *115*, 837.

(39) (a) Hegarty, A. F.; Jencks, W. P. *J. Am. Chem. Soc.* **1975**, *97*, 7188. (b) Jencks, W. P. *Ibid.* **1972**, *94*, 4731.

(40) The  $pK_a$  for quinuclidinone is 11.5 (Table I). The  $pK_a$  for protonation of acetone enolate at oxygen has been determined to be 10.9.<sup>44</sup> The  $pK_a$  for protonation of DHAP enolate at oxygen should be similar because of the offsetting substituent effects of the hydroxyl, which will stabilize the oxyanion inductively, and the phosphate, which will destabilize the oxyanion electrostatically (see text).

(41) Richard, J. P.; Jencks, W. P. *J. Am. Chem. Soc.* **1982**, *104*, 4689.



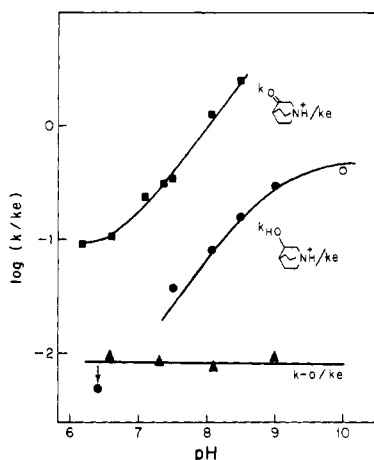
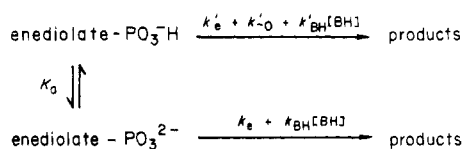


**Figure 7.** The pH dependence of rate constant ratios for partitioning of the enediolate intermediate between protonation at C-1 and leaving group expulsion. The upper curve is for protonation by 3-quinuclidinium ion, the middle curve for protonation by 3-quinuclidinolium ion, and the lower curve for intramolecular protonation by the phosphate monoanion.

#### Scheme IV



LGAP isomerization to DHAP is responsible for the downward curvature observed in plots of  $k_{\text{obsd}}$  against buffer concentration for the LGAP elimination reaction (data not given). This, however, did not noticeably affect the semilogarithmic first-order plots for LGAP reaction because DHAP and LGAP are indistinguishable in our assay and undergo buffer-catalyzed elimination at similar rates (Table I). A theoretical time course of triose phosphate disappearance was determined for LGAP reaction in the presence of 0.80 M quinuclidinone buffer ( $\text{B}/\text{BH} = 4$ , pH 8.1), using pseudo-first-order rate constants for DHAP and LGAP reaction calculated from Table I and a partitioning rate constant ratio calculated from Table III. A semilogarithmic plot of the theoretical data is curved, but the deviation from a straight line drawn through values for the first 3 halftimes of reaction is less than 5%.

The pH-dependence curves for partitioning rate constant ratios are shown in Figure 7. The solid symbols in Figure 7 are from Table III, and the open symbol at pH 10 is the  $k_{\text{BH}}/k_e$  value which best fits the data for Figure 2C. An alternative method is used to obtain the pH 10 value because at this pH the  $\alpha$ -glycerol-phosphate dehydrogenase coupling enzyme used to follow DHAP formation is rapidly inactivated.

A complete analysis of the pH dependence of enediolate partitioning is complicated because the enediolate exists as a mixture of the *cis* and *trans* isomers, the O-1 and O-2 oxyanions, and the phosphate mono- and dianions. However, the data in Figure 7 can be simply explained by the expected differences in the partitioning of the enediolate phosphate monoanion and dianion (Scheme IV). The limiting  $k_{\text{BH}}/k_e$  value at low pH for quinuclidinium reaction is equal to the rate constant ratio for partitioning of the enediolate phosphate monoanion ( $k_{\text{BH}}'/k_e'$  for Scheme IV), and the limiting observed  $k_{\text{BH}}/k_e$  value at high pH for the quinuclidinolium reaction is the rate constant ratio for partitioning of the enediolate phosphate dianion ( $k_{\text{BH}}/k_e$  for Scheme IV). The large increase in  $k_{\text{BH}}/k_e$  with ionization of the phosphate monoanion to the dianion is due primarily to the decrease in the rate constant for leaving group expulsion ( $k_e$ ) for a 5-unit increase in the leaving group  $\text{p}K_a$ ,<sup>42</sup> because the effect

of phosphate ionization on the rate constant for protonation of a carbon 5 atoms removed ( $k_{\text{BH}}$ ) is expected to be small. In the region between pH 7 and 10, where the observed  $k_{\text{BH}}/k_e$  values are increasing, elimination is predominately through the more reactive enediolate phosphate monoanion, and protonation is predominately through the more abundant enediolate phosphate dianion. The observed  $k_{\text{BH}}/k_e$  values increase in this pH range because the concentration of the latter species is increasing relative to that of the former species.

The uncatalyzed protonation of the enediolate with a rate constant  $k_{-O}$  is the microscopic reverse of the uncatalyzed reaction for enediolate formation observed at pH 7–9, i.e., intramolecular protonation of the enediolate by the phosphate monoanion (transition state 3). The observed  $k_{-O}/k_e$  values in Figure 7 are pH independent because both elimination and protonation are predominantly through the enediolate phosphate monoanion.

The line through the points for the 3-quinuclidinium-catalyzed reaction (Figure 7) has been fit by using values of  $k_{\text{BH}}'/k_e' = 0.07$  (the limiting  $k_{\text{BH}}/k_e$  value of low pH),  $k_{\text{BH}}/k_e = 8.4$  (estimated from a limiting  $k_{\text{BH}}/k_e = 0.5$  for 3-quinuclidinolium catalysis, and the ratio  $1.3/0.077$  for observed  $k_{\text{BH}}/k_e$  values for quinuclidinium and quinuclidinolium catalysis at pH 8.1),  $K_a = 10^{-7}$  M for phosphate ionization, and  $k_{\text{BH}}/k_{\text{BH}}' = 1.5$ .<sup>43</sup> The data for 3-quinuclidinolium catalysis have been fit similarly:  $k_{\text{BH}}'/k_e' = 0.004$ ,  $k_{\text{BH}}/k_e = 0.5$ ,  $K_a = 10^{-7}$  M, and  $k_{\text{BH}}/k_{\text{BH}}' = 1.5$ .

Rate constants  $k_{\text{BH}}$  for buffer protonation of the enediolate at C-1 can be calculated from the rate constants for buffer-catalyzed DHAP deprotonation and an estimated  $\text{p}K_a$  for deprotonation. This  $\text{p}K_a$  is expected to be similar to the  $\text{p}K_a$  of 19.2<sup>44</sup> for acetone deprotonation because the effects of the DHAP hydroxyl and phosphate substituents will tend to offset one another.

The hydroxyl group of DHAP will stabilize the carbanion by an inductive effect,<sup>45,46</sup> and possibly by intramolecular hydrogen bonding to the C-2 oxyanion in the *cis*-enediolate. There are also less important destabilizing interactions between the carbanion and the lone pairs of electrons at oxygen.<sup>46</sup> Substitution of a hydroxyl group for a hydrogen has been found to increase the rate constants for ethoxide-catalyzed detritiation of carbon acids in ethanol by 200–500-fold.<sup>45</sup>

The phosphate dianion will destabilize the carbanion due to electrostatic destabilization of the enediolate oxyanion. These same destabilizing electrostatic interactions cause the 1-unit increase in  $\text{p}K_a$  for ionization of the enediolate phosphate monoanion ( $\text{p}K_a = 7$ , Figure 7) over the  $\text{p}K_a$  for ionization of LGAP phosphate monoanion ( $\text{p}K_a = 6$ , Figure 1).

The observed rate constants for the hydroxide-catalyzed deprotonation of DHAP and acetone are  $0.56 \text{ M}^{-1} \text{ s}^{-1}$ <sup>18</sup> (at 37 °C) and  $0.25 \text{ M}^{-1} \text{ s}^{-1}$ <sup>19</sup> (at 25 °C), respectively. The value of the former will be increased 3-fold relative to the latter by a statistical correction (there are 2 and 6 equivalent protons respectively for the hydroxide-catalyzed deprotonation of DHAP and acetone) and may be changed relative to the latter by a temperature effect. Overall the offsetting substituent effects lead to a relatively small increase in  $k_{\text{OH}^-}$  for DHAP compared to acetone deprotonation, suggesting that the DHAP carbanion is slightly more stable than the acetone carbanion. Accordingly a  $\text{p}K_a$  of 18 is estimated for DHAP ionization at carbon-3. Combining this  $\text{p}K_a$  and the rate constants for buffer-catalyzed deprotonation of DHAP gives

(43) The electrostatic destabilization of the enediolate phosphate dianion compared to enediolate phosphate monoanion which was proposed as the explanation for the smaller quinuclidinone  $k_B$  values for formation of the more unstable enediolate phosphate dianion also accounts for the larger  $k_{\text{BH}}$  than  $k_{\text{BH}}'$  values for protonation of these species. The fit for the data in Figure 7 to a  $k_{\text{BH}}/k_{\text{BH}}'$  value of 1.5 is substantially better than the fit for values of 1 or 2.

(44) Chiang, Y.; Kresge, A. J.; Tang, Y. S.; Wirz, J. J. *Am. Chem. Soc.* **1984**, *106*, 460.

(45) Thomas, P. J.; Stirling, C. J. M. *J. Chem. Soc., Perkins Trans.* **1977**, 1909.

(46) (a) Hine, J. In "Structural Effects on Equilibria in Organic Chemistry"; Wiley-Interscience: New York, 1975; p 181. (b) Hine, J.; Langford, P. B. *J. Am. Chem. Soc.* **1956**, *78*, 5002. (c) Hine, J.; Dalsin, P. D. *J. Am. Chem. Soc.* **1972**, *94*, 6998.

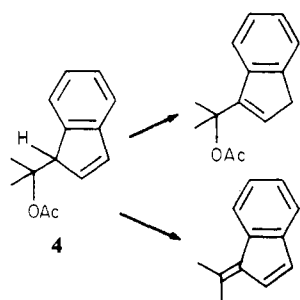
(42) (a) Crosby, J.; Stirling, C. J. M. *J. Chem. Soc. B* **1970**, 679. (b) Ogata, Y.; Sawaki, Y.; Isono, M. *Tetrahedron* **1970**, *26*, 3045. (c) Friedman, M.; Cavins, J. F.; Wall, J. S. *J. Am. Chem. Soc.* **1965**, *87*, 3672.

calculated rate constants of  $1.0 \times 10^8$  and  $6.1 \times 10^6 \text{ M}^{-1} \text{ s}^{-1}$  respectively for quinuclidinonium- and quinuclidinium-catalyzed protonation of the enediolate phosphate dianion at C-1. Rate constants of  $8 \times 10^8$  and  $8 \times 10^6 \text{ s}^{-1}$  respectively for leaving group expulsion from the enediolate phosphate monoanion and dianion are calculated from

$$k_e = k_{\text{BH}}(k_e/k_{\text{BH}})_{\text{obsd}}(f_{\text{C-2 oxyanion}}/f_{\text{C-1 oxyanion}})$$

which corrects (by <2 fold)<sup>47</sup> the limiting  $k_{\text{BH}}/k_e$  and  $k_{\text{BH}}'/k_e'$  values at high and low pH (Figure 7) for a slightly greater concentration of the species which expels a leaving group (C-1 oxyanion) over the species which is protonated (C-2 oxyanion). The  $k_e'/k_e$  of 100 gives a  $\beta_{1g}$  of -0.4 for leaving group expulsion based on points for phosphate dianion and trianion leaving groups. This is similar to estimated  $\beta_{1g}$  values for related systems.<sup>21,42</sup>

Concurrent aldose-ketose isomerization and  $\beta$ -elimination reactions of triose phosphates through a common enediolate intermediate are reminiscent of the concurrent 1,3-isomerization and 1,2-elimination reactions of 1-(1-acetoxy-1-methylethyl)indene (4) through a common carbanion intermediate.<sup>48</sup> In the latter



case intramolecular proton transfer was observed for the isomerization reaction, in part because the reaction was in methanol where ion pairs have fair stabilities. Here the enediolate must be protonated by a solvent-derived proton since there is a large solvent deuterium isotope effect on  $k_{\text{BH}}$ . The absence of significant intramolecular proton transfer shows that the rate constant for diffusional separation of the acid-enediolate ion pair ( $10^{10} \text{ s}^{-1}$ )<sup>49</sup> is larger than the rate constant for acid protonation of the enediolate and is consistent with our estimated rate constants for general acid protonation.

#### Comparison of the Nonenzymatic and the Enzymatic Reactions.

There is a greater diversity of pathways for reaction of triose phosphates in water, compared to the stereospecific reactions catalyzed by triose phosphate isomerase and methylglyoxal synthase. In solution the enediolate freely partitions between elimination and protonation, while the enzymatic reactions are specific for either elimination or protonation. The specificity of TPI for proton-transfer reactions is probably achieved by binding the substrate in a conformation that places the phosphate-oxygen bond to C-3 in the plane of the intermediate<sup>50</sup> in order to minimize the overlap between the  $\pi$  system of the enediolate and the orbital formed upon cleavage of the bond at C-3. It is likely that methylglyoxal synthase binds the enediolate in an alternative con-

**Table IV.** Comparison of the Rate Constants for Quinuclidinone and Enzymatic Catalysis of Triose Phosphate Isomerization of DHAP at 37 °C

	quinuclidinone	triose phosphate isomerase <sup>a</sup>
$K_d^1$ , M	21	$6.2 \times 10^{-4b}$
$k_1$ , $\text{s}^{-1}$	$2.2 \times 10^{-2}$	$1.1 \times 10^4$
$k_{-1}$ , $\text{s}^{-1}$	$6.9 \times 10^8$	$8.6 \times 10^4$
$k_2$ , $\text{s}^{-1}$	$5.2 \times 10^7$	$1.1 \times 10^5$
$k_{-2}$ , $\text{s}^{-1}$	$4.0 \times 10^{-1}$	$1.0 \times 10^4$
$K_d^2$ , M	230	$3.2 \times 10^{-4b}$
$k_{\text{cat}}$ (DHAP $\rightarrow$ GAP), $\text{s}^{-1}$	$1.5 \times 10^{-3c}$	1300
$k_{\text{cat}}/K_m$ (DHAP $\rightarrow$ GAP), $\text{M}^{-1} \text{ s}^{-1}$	$7.3 \times 10^{-5}$	$2.1 \times 10^6$

<sup>a</sup> Calculated from data in ref 54. <sup>b</sup> Kinetic  $K_m$  values for the enzyme from rabbit muscle.<sup>23</sup> <sup>c</sup>  $k_1 k_2 / (k_{-1} + k_2)$ .

figuration, with the phosphate-oxygen bond to carbon perpendicular to the plane of the enediolate, in order to maximize orbital overlap.<sup>3</sup> Protonation of an enzyme-bound enediolate could account for the triose phosphate isomerase catalyzed elimination reaction at pH <7<sup>51</sup> because conversion of the enediolate phosphate dianion to the monoanion favors the partitioning to elimination products.

There are separate pathways in solution for intramolecular, solvent-catalyzed, and buffer-catalyzed deprotonation of triose phosphates. The intramolecular pathway observed at pH <10 has been proposed to occur in aldolase catalysis;<sup>20</sup> however, there is no compelling reason to favor intramolecular over direct deprotonation by a catalytic base of the enzyme. There is no more than a small kinetic advantage for the intramolecular pathway because in solution the reactivity of the substrate phosphate is only marginally greater (0.7–2-fold) than 1 M of added base with a similar  $pK_a$ . In fact the first-order rate constant for phosphate deprotonation in the intramolecular reaction is smaller than the estimated first-order rate constant for deprotonation by a comparably basic buffer in a loose association complex with substrate, because (assuming an association complex of  $0.1 \text{ M}^{-1}$  for complex formation)<sup>52</sup> at 1 M buffer the concentration of the buffer-substrate complex is only 10% that of the total substrate, whereas every triose phosphate molecule contains a phosphate base.

The intramolecular pathway has the disadvantage that it limits binding interactions between the enzyme and substrate phosphate in the transition state for deprotonation, and in the case of triose phosphate isomerase is probably sterically prohibited by restriction of the phosphate-oxygen bond to C-3 to the plane of the enediolate intermediate. Intramolecular deprotonation may be favored for the elimination reaction catalyzed by methylglyoxal synthase because the product of proton transfer has the phosphate leaving group in the more reactive monoanionic form. However, this should not be an important factor since the uncatalyzed leaving group expulsion from the enediolate phosphate dianion is already very fast ( $8 \times 10^6 \text{ s}^{-1}$ ) relative to  $k_{\text{cat}}$  for the enzymatic reaction ( $10 \text{ s}^{-1}$ ).<sup>3</sup>

Figure 5 shows that general bases are better catalysts of triose phosphate deprotonation for their  $pK_a$  than is hydroxide because of the large deviation of hydroxide from the Brønsted correlation for general base catalysis and because of the shallow slope ( $\sim 0.5$ ) of this correlation.<sup>53</sup> These factors will favor proton transfer to a general base at the enzyme over enzymatic catalysis of the hydroxide reaction. In addition, the substrate at the enzyme has a greatly enhanced reactivity compared to its reactivity in an encounter complex with a general base as shown by the rate constants in Table IV for quinuclidinone (rate constants for eq 8) and triose phosphate isomerase catalyzed isomerization.<sup>54</sup>

(47) A larger concentration of O-1 than O-2 oxyanion is assumed because electrostatic destabilization of the negative charge will be weakest when the charge is at the oxygen furthest removed from the negatively charged phosphate. The ratios of 0.77 and 0.62 for O-2/O-1 anion concentrations are based on estimated  $pK_a$  differences for deprotonation of the C-1 and C-2 hydroxyls of 0.1 and 0.2 respectively for the enediol phosphate mono- and dianions. The difference for the enediol phosphate monoanion is based on the 0.1 unit difference in the second  $pK_a$ s for dicarboxylic acids separated by 4 and 5 atoms. A twofold larger difference is estimated for the enediol phosphate dianion because the energy of electrostatic destabilization depends on the product of the interacting charges (ref 46a, p 30). This estimate is only approximate, but it suggests that only a small correction of the observed values is needed.

(48) (a) Thibblin, A.; Bengtsson, S.; Ahlberg, P. *J. Chem. Soc., Perkins Trans.* 2 1977, 1569. (b) Thibblin, A.; Ahlberg, P. *J. Am. Chem. Soc.* 1979, 101, 7311. (c) Thibblin, A.; Ahlberg, P. *Ibid.* 1977, 99, 7926.

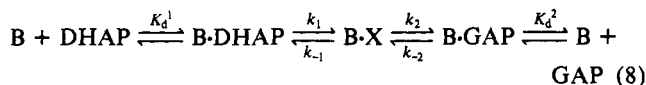
(49) Estimated by using a rate constant of  $10^9 \text{ M}^{-1} \text{ s}^{-1}$  for diffusion-controlled encounter-complex formation (Eigen, M. *Angew. Chem., Int. Ed. Engl.* 1964, 3) and an encounter-complex association constant of  $0.1 \text{ M}^{-1}$ .<sup>52</sup>

(50) Alber, T.; Banner, D. W.; Bloomer, A. C.; Petsko, G. A.; Phillips, D.; Rivers, P. S.; Wilson, I. A. *Philos. Trans. R. Soc. London, Ser. B* 1981, 293, 159.

(51) Iyengar, R.; Rose, I. A. *Biochemistry* 1981, 20, 1223.

(52) Davies, C. S. "Ion Association"; Butterworths: London, 1962; pp 77–87.

(53) Jencks, W. P. *Acc. Chem. Res.* 1976, 9, 425.



Values for the nonenzymatic reaction were calculated for the reaction of the carbonyl form of the substrate from the following: the rate constants for buffer-catalyzed elimination (rate-determining protonation), a  $pK_a$  of 18 for deprotonation of DHAP at carbon, a  $K_d$  of 10 M for breakdown of the buffer-substrate encounter complex,<sup>52</sup> values of 0.32<sup>23</sup> and 0.043<sup>24</sup> respectively for the fraction of DHAP and GAP present in the carbonyl form, and an equilibrium constant of 1/22 for isomerization.<sup>38</sup>

The comparison of the rate constants in Table IV for the nonenzymatic and the enzymatic reactions is made with the assumption that the same intermediate is formed in solution and at the enzyme, i.e., the enediolate. This is supported by crystallographic data for the E-DHAP complex because there is apparently no enzymic general acid available to protonate the enediolate oxyanion.<sup>50</sup> If the enzymatic reaction is through an enediol intermediate then the acceleration of deprotonation relative to the *same mechanism* in solution must be considerably larger than the deprotonation ratio in Table IV, because the third-order rate constant for buffer catalysis of enediol formation through a termolecular transition state containing a molecule of buffer acid and buffer base is too small to be experimentally significant.

It would be most informative to compare the reactivity of TPI with that of a small buffer with the same  $pK_a$  as the catalytic base at the active site during turnover, but this  $pK_a$  is not known. Glu 165 at the active site of the rabbit muscle enzyme<sup>50</sup> is alkylated by glycidol phosphate with a pH dependence consistent with a  $pK_a \leq 5.5$ .<sup>55</sup> However, the binding of the intermediate analogue phosphoglycolate to the enzyme from yeast changes the  $pK_a$  of a residue which may be the catalytic base.<sup>56d</sup> The  $pK_a$  for protonation of an enzyme residue at the E-phosphoglycolate complex, 6.7, is close to the  $pK_a$  of 7.5 for quinuclidinone. We favor the higher  $pK_a$  value for the catalytic residue because this will give the enzyme an increased reactivity for substrate deprotonation.

A ( $3 \times 10^{10}$ )-fold enzymatic acceleration of  $k_{cat}/K_m$  is calculated from the data in Table IV which can be further divided into a  $3 \times 10^5$  decrease in  $K_m$  and a  $9 \times 10^5$  increase in  $k_{cat}$ . The decreased  $K_m$  value is reflected by increased levels of E-DHAP complexes compared to B-DHAP complexes at low catalyst concentrations. The increased  $k_{cat}$  value is due in small part to a more favorable partitioning of the intermediate to products in the enzymatic reaction and primarily to a  $5 \times 10^5$  increase in the reactivity of the substrate toward deprotonation by a general base when bound to the enzyme compared to deprotonation by a small base in water. There is also a large increase in the stability of

the enzyme bound enediol intermediate; the ratio  $k_1/k_{-1}$  is 0.13 for the enzymatic reaction and  $3 \times 10^{-11}$  for the nonenzymatic reaction.<sup>57</sup> Thus the factors responsible for the  $10^{10}$ -fold stabilization of the intermediate on the enzyme will bring about a ( $5 \times 10^5$ )-fold deprotonation rate acceleration if they are partially ( $\sim 50\%$ ) expressed in the transition state for enzymatic deprotonation.

There is a direct correlation between intermediate stabilization on the enzyme and the relative affinities of enzyme for intermediate and substrate; i.e., the  $10^{10}$ -fold stabilization of the intermediate corresponds to a  $10^{10}$ -fold tighter affinity of the enzyme for intermediate compared to substrate DHAP. This is consistent with the observed high affinity of the enzyme for the intermediate analogue phosphoglycolate.<sup>56</sup> The difference between the substrate and intermediate binding energies may be due to a destabilizing interaction expressed in substrate, but not intermediate, binding (e.g., substrate deformation to a planar configuration) or a stabilizing interaction expressed in intermediate, but not substrate, binding (e.g., electrostatic stabilization of the C-1 and C-2 oxyanions).<sup>50,58</sup> The differential binding of substrate and intermediate will lead to an increase in  $k_{cat}$  if the intermediate binding energy is also expressed in the binding of the transition state for intermediate formation. The part of the intermediate binding energy which is expressed in binding of the reaction transition state, but not substrate, is "utilized" to stabilize the reaction transition state.<sup>59</sup>

**Acknowledgment.** This work was supported by United States Public Health Grants GM-20940, CA-06927, and RR-05539 and by an appropriation from the Commonwealth of Pennsylvania. I thank Dr. Sam Litwin for determining the theoretical time course for LGAP reaction and Dr. Irwin Rose for his support.

**Note Added in Proof.** I have learned since the acceptance of this manuscript that the rate constants in Table IV (from ref 54) for the triose phosphate isomerase catalyzed reaction were calculated from experimental results which are now known to be flawed (Dr. Irwin A. Rose, manuscript submitted for publication to *Biochemistry*). However, since the enzymatic rate constants in Table IV are similar to the values previously published by Albery and Knowles,<sup>60</sup> the major points raised in the discussion of Table IV remain valid.

**Registry No.** L-Glyceraldehyde 3-phosphate, 20283-52-7; phosphate dianion, 10030-20-3; quinuclidine, 100-76-5; 3-hydroxyquinuclidine, 1619-34-7; 3-chloroquinuclidine, 42332-45-6; 3-ketoquinuclidine, 3731-38-2;  $OH^-$ , 14280-30-9;  $CF_3CH_2O^-$ , 24265-37-0;  $N(CH_2CH_3)_3$ , 121-44-8;  $CO_3^{2-}$ , 3812-32-6;  $N(CH_2CH_2OH)_3$ , 102-71-6.

(54) Calculated from partition ratios: Rose, I. A.; Iyengar, R. *Biochemistry* **1982**, *21*, 1591. A twofold difference in  $k_{cat}$  was assumed for reactions at 23 and 37 °C.

(55) (a) Schray, K. J.; O'Connell, E. L.; Rose, I. A. *J. Biol. Chem.* **1973**, *248*, 2214. (b) Waley, S. J. *Biochem. J.* **1972**, *126*, 255.

(56) (a) Wolfenden, R. *Biochemistry* **1970**, *9*, 3404. (b) Johnson, L. N.; Wolfenden, R. *J. Mol. Biol.* **1970**, *47*, 93. (c) Hartman, F. C.; LaMuraglia, G. M.; Tomozawa, Y.; Wolfenden, R. *Biochemistry* **1975**, *14*, 5274. (d) Wolfenden, R. In "Antimetabolites in Biochemistry Biology and Medicine"; Skoda, J.; Langen, P., Eds.; Pergamon Press: Oxford, 1979; Vol. 57, pp 151-160.

(57) To a first approximation the buffer-independent equilibrium constant for DHAP tautomerization to the enediol will be the value of  $10^{-8}$  observed for acetone.<sup>44</sup> This is also substantially smaller than the equilibrium constant of 0.13 for intermediate formation at the enzyme.

(58) (a) Belasco, J. G.; Knowles, J. R. *Biochemistry* **1980**, *19*, 472. (b) Webb, M. R.; Knowles, J. R. *Biochem. J.* **1974**, *141*, 589.

(59) (a) Jencks, W. P. In "Advances in Enzymology"; Meister, A., Ed.; John Wiley and Sons: New York, 1975; Vol. 43, pp 219-410. (b) Jencks, W. P. In "Molecular Biology, Biochemistry and Biophysics"; Chapeville, F.; Haenni, A. L., Eds.; Springer-Verlag: New York, 1980; Vol. 32, pp 3-25.

(60) (a) Albery, W. J.; Knowles, J. R. *Biochemistry* **1976**, *15*, 5627. (b) Albery, W. J.; Knowles, J. R. *Acc. Chem. Res.* **1977**, *10*, 105.